High-Rayleigh-number convection in spherical shells

A. Tilgner
Physikalisches Institut, Universität Bayreuth, D-95440 Bayreuth, Germany
(Received 5 October 1995; revised manuscript received 27 December 1995)

Convection in a self-gravitating spherical shell is simulated numerically for Prandtl numbers between 10 and 0.06. This geometry introduces asymmetries between the boundary layers whose influence on the scaling properties of the Nusselt and Reynolds numbers is investigated. The observed Prandtl number dependences are compared with predictions from mixing length theory and more recent theories which describe the ''hard turbulence'' regime of convection. [S1063-651X(96)03605-7]

PACS number(s): 47.27.Te, 92.60.Ek

Convection at high Rayleigh numbers (Ra) has received much interest in the recent past due to the discovery of several simple scaling relationships between relevant quantities, and a classification of turbulent states according to statistical properties into ''soft'' and ''hard'' turbulence [1]. Perhaps the most notorious of the scaling laws is the dependence of the Nusselt number (Nu) on Ra, which behaves as $\mathrm{Ra}^{2/7}$. This observation contradicts an early theory according to which the boundary layers are marginally stable [2]. The 2/7 law could be accounted for by a scaling theory based mostly on dimensional arguments [3]. Further experiments however revealed the existence of a large-scale flow which was only taken into consideration by a later theory [4]. There is evidence that the 2/7 law even holds when gravity and the applied temperature gradient are perpendicular to each other [5]. It therefore becomes interesting to inquire under which conditions this scaling is violated. The behavior of Nu is connected to the variation of the circulation velocity. It also seems promising to study the modifications of the situation realized in laboratory experiments which might influence the scaling properties of this circulation in order to investigate its nature.

While the Ra dependence of convection has been thoroughly studied both experimentally and numerically, much less is known about the Prandtl number (Pr) dependence [6]. Experiments of course have to rely on available fluids, but in numerical work, Pr can conveniently be varied.

This paper presents results on convection in a self-gravitating spherical shell with a special emphasis on the Pr dependence. Comparison will be made with experiments in planar geometry. Convection in a spherical shell is of obvious relevance to geo- and astrophysics. From a more fundamental point of view, the problem sheds light on the influence of asymmetries between the hot and cold surface: In a shell, the inner (hot) surface is of a smaller area than the outer (cold) boundary. Also, the radius of curvature of the, say, inner sphere introduces a new length scale in addition to the separation of the hot and cold boundaries. In a self-gravitating fluid, gravitational acceleration increases with radius, creating an additional asymmetry. Previous numerical studies of convection in spherical shells [7] have focused on high Pr and emphasized the flow patterns, whereas scaling relations received little attention.

Only an overview of the numerical method is given here since full details will be presented in a forthcoming publication [8]. The model treats a fluid contained in a spherical shell of inner and outer radii r_i and r_o with $r_i/r_o=0.4$. This ratio has been chosen to agree with the geometry of the earth's liquid core. Gravity is assumed to vary linearly with radius corresponding to an inner core of the same density as the fluid. The boundaries are impermeable, no slip and at constant temperatures. Convection is described in the Boussinesq approximation by Eqs. (1)–(3) for the velocity $\mathbf{u}$ and the temperature T:

$$\frac{\partial}{\partial t}\boldsymbol{\nabla}\times\mathbf{u}+\boldsymbol{\nabla}\times[(\boldsymbol{\nabla}\times\mathbf{u})\times\mathbf{u})]=\frac{\mathrm{Ra}}{r_o}\boldsymbol{\nabla}\times(T\mathbf{r})+\nabla^2\boldsymbol{\nabla}\times\mathbf{u}, \tag{1}$$

$$\boldsymbol{\nabla}\cdot\mathbf{u}=0, \tag{2}$$

$$\frac{\partial}{\partial t}T+\mathbf{u}\cdot\boldsymbol{\nabla}T=\frac{1}{\mathrm{Pr}}\nabla^2T. \tag{3}$$

The problem has been made nondimensional by using the gap width $d=r_o-r_i$ as the length scale, d^2/ν as the time scale, and $\mathrm{Pr}\Delta T$ as the temperature scale, where the Prandtl number Pr is defined by $\mathrm{Pr}=\nu/\kappa$, ν and κ being the momentum and thermal diffusivities. ΔT is the temperature difference between the inner and outer spheres. The Rayleigh number Ra is given by

$$\mathrm{Ra}=\frac{g_o\alpha\Delta T d^3}{\kappa\nu}, \tag{4}$$

with g_o being the gravitational acceleration at the outer surface and α the thermal expansion coefficient. The temperature is decomposed as $T=T_s+\Theta$ where Θ stands for the temperature deviation from the pure conduction profile T_s,

$$T_s=-\frac{1}{\mathrm{Pr}}\frac{1-r_i/r}{1-r_i/r_o}. \tag{5}$$

The solenoidal velocity field is written in terms of the poloidal and toroidal scalars v and w

$$\mathbf{u}=\boldsymbol{\nabla}\times\boldsymbol{\nabla}\times(v\mathbf{r})+\boldsymbol{\nabla}\times(w\mathbf{r}). \tag{6}$$

The resulting equations for v, w, and Θ are solved with a pseudospectral method using Chebyshev polynomials for the radial direction and spherical harmonics for the angles. Time

 © 1996 The American Physical Society

TABLE I. Pr, Ra, number of radial collocation points n_r, maximum order of spherical harmonics L, Nu, Re, and boundary layer thicknesses D normalized by the shell thickness d (subscripts i,o denote inner and outer boundary, subscripts v,T denote velocity and temperature layer) for all calculations. Runs at different resolutions are compared at $\mathrm{Ra}=8\times10^4$ for Pr=0.1, 1 and 10. Errors can be estimated from results obtained by averaging over different stretches of time, starting from different initial conditions and using different resolutions. The errors on Nu are typically a few units on the last digit given in the table (but less than ±0.1), at most 10% on Re and about ±0.015 on the boundary layer thicknesses. At lower Pr, a higher Ra needs to be reached before the temperature profile is significantly disturbed from its static shape [Eq. (5)]. For this reason, the error on $D_{o,T}$ is about ±0.05 at $\mathrm{Ra}=8\cdot10^4$, Pr=0.1 and 0.06. Values for $D_{i,T}$ or $D_{o,T}$ are only given if a boundary layer can be clearly discerned at the inner or outer sphere.

Pr	Ra	n_r	L	Nu	Re	$D_{i,v}/d$	$D_{o,v}/d$	$D_{i,T}/d$	$D_{o,T}/d$
0.06	$8\cdot10^4$	33	64	2.15	264	0.103	0.097	0.187	0.224
0.1	$4\cdot10^3$	33	32	1.0559	19.5	0.178	0.177		
0.1	$5\cdot10^3$	33	32	1.1173	29.3	0.180	0.154		
0.1	$1\cdot10^4$	33	32	1.39	70	0.161	0.133		
0.1	$2\cdot10^4$	33	32	1.74	102	0.142	0.135	0.271	
0.1	$5\cdot10^4$	33	32	2.05	147	0.117	0.121	0.194	
0.1	$8\cdot10^4$	17	32	2.26	182	0.110	0.117	0.176	0.227
0.1	$8\cdot10^4$	33	32	2.31	180	0.109	0.126	0.175	0.299
0.1	$8\cdot10^4$	33	64	2.27	190	0.120	0.105	0.169	0.246
0.1	$1\cdot10^5$	33	32	2.37	197	0.108	0.109	0.164	0.266
0.3	$8\cdot10^4$	33	32	2.54	81	0.130	0.127	0.151	0.187
0.6	$8\cdot10^4$	33	32	2.75	50	0.137	0.137	0.138	0.157
1	$4\cdot10^3$	17	32	1.276	3.07	0.189	0.210		
1	$5\cdot10^3$	33	32	1.435	6.36	0.191	0.207		
1	$1\cdot10^4$	33	32	1.833	11.9	0.19	0.187	0.252	
1	$2\cdot10^4$	33	32	2.033	13.9	0.183	0.167	0.226	0.247
1	$5\cdot10^4$	33	32	2.546	25.6	0.163	0.157	0.156	0.177
1	$8\cdot10^4$	17	32	2.85	33.2	0.147	0.147	0.136	0.147
1	$8\cdot10^4$	33	32	2.88	33.3	0.145	0.145	0.133	0.144
1	$8\cdot10^4$	33	64	2.90	34.0	0.143	0.148	0.127	0.157
1	$1\cdot10^5$	33	64	3.0	37.4	0.138	0.142	0.118	0.144
1	$2\cdot10^5$	33	64	3.6	52.7	0.119	0.120	0.0973	0.111
1	$4\cdot10^5$	33	64	4.05	71.8	0.109	0.101	0.0843	0.0827
1	$8\cdot10^5$	65	64	5.0	100	0.093	0.090	0.069	0.062
3	$8\cdot10^4$	17	32	2.84	11.7	0.163	0.147	0.138	0.127
6	$8\cdot10^4$	17	32	2.82	6.32	0.173	0.161	0.138	0.127
10	$4\cdot10^3$	17	16	1.298	0.490	0.195	0.211		
10	$5\cdot10^3$	17	16	1.461	0.69	0.196	0.207		
10	$1\cdot10^4$	17	16	1.882	1.32	0.194	0.197	0.265	0.301
10	$2\cdot10^4$	17	16	2.246	2.12	0.190	0.186	0.201	0.209
10	$4\cdot10^4$	17	32	2.47	2.68	0.185	0.188	0.169	0.173
10	$8\cdot10^4$	17	32	2.82	4.0	0.175	0.171	0.139	0.128
10	$8\cdot10^4$	33	32	2.82	4.0	0.175	0.171	0.137	0.128
10	$2\cdot10^5$	17	81	3.50	6.63	0.168	0.163	0.106	0.111
10	$4\cdot10^5$	17	81	4.03	9.59	0.160	0.156	0.090	0.092
10	$8\cdot10^5$	17	81	4.85	13.8	0.158	0.156	0.079	0.077

stepping is performed with the Adams-Bashforth scheme for the buoyancy and advection terms coupled to a Crank-Nicholson step for the diffusion terms. The maximum resolution used in this work was 65 radial collocation points and spherical harmonics of an order up to 64, corresponding to a total of 5.4×10^5 grid points. The simulation was restricted to flows symmetric to a meridional plane.

A summary of the data to be discussed is given in Table I. Figure 1 shows the Ra dependence of Nu for Pr=0.1, 1, and 10. The onset of convection occurs in this model at Ra =2847. Figure 1 also includes the experimentally determined Nu(Ra) at Pr=0.7 in a cell of aspect ratio 6.7 [9,10], which follows a $\mathrm{Ra}^{2/7}$ scaling at $\mathrm{Ra}>5\times10^3$. It is seen from Fig. 1 that the scaling in the spherical model deviates significantly from the one observed in planar convection and that the exponent in the former is less than 2/7 (approximately 0.24).

Figure 2 shows the Reynolds number (Re) for the spherical model as a function of Ra. Re was computed with the maximum value of the rms of the radial velocity fluctuations

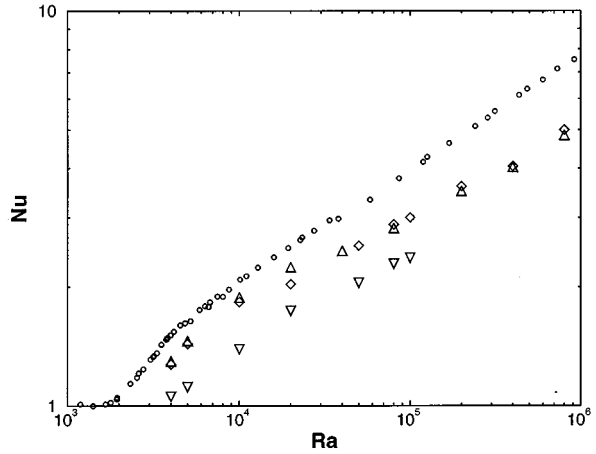

FIG. 1. Nu as a function of Ra for Pr=0.1 (triangle down), 1 (diamonds), and 10 (triangle up). The circles are experimental measurements on a cell of aspect ratio 6.7 at Pr=0.7 (numbers taken from Ref. [10]).

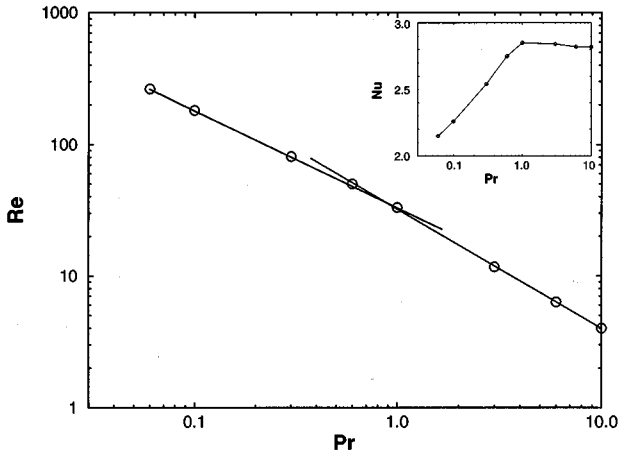

FIG. 3. Re as a function of Pr at Ra=$8\cdot10^4$. The straight lines correspond to exponents −0.73 (low Pr) and −0.92 (high Pr). The inset shows the variation of Nu.

averaged over a spherical surface and time. This maximum occurs at $r/d=1.1\pm0.05$ independently of Ra and Pr. The solid lines in Fig. 2 correspond to an exponent of 0.5, which is the exponent found for a best fit to the Pr=1 data. These lines fit all results to within errors, although the exponent of the best fit to the data varies from 0.53 for Pr=10 to 0.47 for Pr=0.1.

In order to further explore the Pr dependence, an additional series of runs was performed at a constant Ra of 8×10^4, which was chosen to lie within the range of validity of the power laws in Figs. 1 and 2. Nu and Re are given as a function of Pr in Fig. 3. Both quantities indicate a change of regime around Pr=1, where the Nu goes through a weak maximum and appears to asymptote to a constant at a high Pr. Re is decreasing with a larger exponent at Pr>1 than at Pr<1. At this particular Ra, states at Pr<1 are chaotic or turbulent, states at Pr=1 and 3 are oscillatory, whereas flows at Pr=6 and 10 are steady.

The asymmetry between the inner and outer surfaces leads to a dramatic asymmetry in the temperature profile with a larger temperature drop at the inner boundary. The temperature at midshell normalized by the applied temperature difference $T_c/\Delta T$ varies from −0.82 at Pr=0.06, Ra=$8\cdot10^4$ to −0.88 at Pr=10, Ra=8×10^5. In this second case, only 12% of the total temperature drop occurs at the outer boundary. The general trend is that $T_c/\Delta T$ decreases with increasing Ra and Pr.

Next we investigate the behavior of the temperature and velocity boundary layers. The boundary layer thicknesses are determined by locating the radius at which the temperature and horizontal velocity fluctuations averaged over a spherical surface have a local maximum. Their variation with Pr and Ra are shown in Figs. 4 and 5. The thermal boundary layer thickness exceeds the viscous one at a low Ra and Pr. The thicknesses of the inner and outer viscous layers are nearly equal at all Ra and Pr. The local Reynolds number of the inner velocity boundary layer exceeds by typically 20% the one at the outer sphere. The local Rayleigh number of the

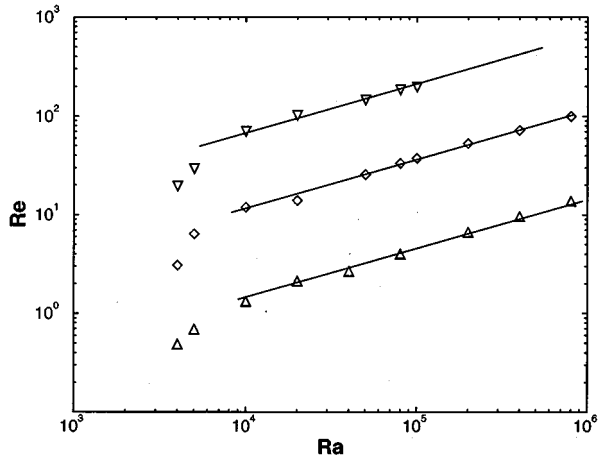

FIG. 2. Re as a function of Ra for Pr=0.1 (triangle down), 1 (diamonds), and 10 (triangle up). The straight lines correspond to an exponent of 0.5.

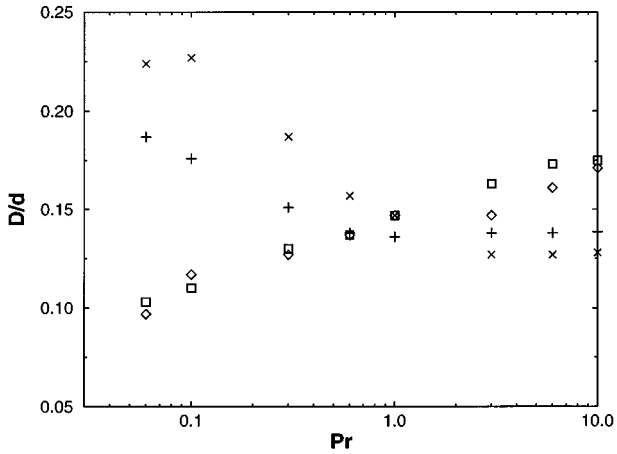

FIG. 4. Variation of the boundary layer thicknesses D, normalized by the shell thickness d, with Pr at Ra=8×10^4. The cross and plus represent the thermal boundary layer thickness at the outer and inner sphere, respectively. Diamonds and squares represent the viscous boundary layer thickness at the outer and inner sphere, respectively.

temperature boundary layers is always less than 150, i.e., far from critical.

Asymmetric thermal boundary layers have been studied experimentally by Wu and Libchaber in non-Boussinesq convection [11]. In that case, the thermal boundary layers scales associated with the boundary layers ($\kappa\nu/g\alpha\lambda^3$, where λ is the boundary layer thickness) is independent of Ra. This does not happen in the spherical model, nor does any other of the simple conditions proposed in Ref. [11] hold at all Ra and Pr.

Let us discuss a few theories originally developed for the planar geometry. It has been proposed [3,12] that Re is connected to the free fall velocity $(g\alpha d\theta)^{1/2}$ where θ is a characteristic temperature scale. If we use the applied temperature difference ΔT for θ, we obtain $\mathrm{Re}\propto\mathrm{Ra}^{1/2}\mathrm{Pr}^{-1/2}$. An alternative is to use the rms of the temperature fluctuations in the center. For numerical purposes, less noisy data are obtained if we use the temperature fluctuations averaged over the entire shell. This quantity, normalized by ΔT, shows very little Pr dependence ($\mathrm{Pr}^{-\alpha}$ with $\alpha<0.07$). We conclude that the free fall hypothesis does not quantitatively reproduce the correct Pr dependence of the Re.

Another theory by Shraiman and Siggia [4], which is successful in predicting the 2/7 scaling of Nu in the planar geometry, rests on the assumption that the boundary layers are turbulent with a logarithmic velocity profile. In the present simulations, the Reynolds numbers of the velocity boundary layers are always less than 15. Thus it comes as no surprise that the Pr dependence proposed in Ref. [4] ($\mathrm{Re}/\ln\mathrm{Re}\propto\mathrm{Pr}^{-5/7}$) is not verified in our numerical results.

Both Ref. [3] and the theory by Shraiman and Siggia predict a Nu monotonically decreasing with an increasing Pr at a constant Ra, which we do not observe numerically [13].

Finally, we consider the mixing length theory by Kraichnan [14]. According to this theory, Nu goes as $\mathrm{Pr}^{1/3}\mathrm{Ra}^{1/3}$ at low Pr and as $\mathrm{Ra}^{1/3}$ (independent of Pr) at high Pr, whereas Re varies as $\mathrm{Pr}^{-5/9}\mathrm{Ra}^{4/9}$ at low Pr and as $\mathrm{Pr}^{-2/3}\mathrm{Ra}^{4/9}$ at high Pr. These relations are restricted to a Ra low enough so that the velocity layers are not turbulent and do not develop a logarithmic profile. The distinction between ''low'' and ''high'' Pr arises from the relation between the thicknesses of the viscous and thermal boundary layers: At ''low'' Pr, the viscous boundary layer is thinner than the thermal one. The crossover was somewhat arbitrarily expected to occur at Pr=0.1. Qualitative agreement is found with our simulations in the sense that Nu indeed rises at low Pr and reaches a constant level at a high Pr, and Re decreases more slowly with increasing Pr at a low rather than at high Pr. The separation between these regimes is at Pr≈1, where the boundary layers change their hierarchy (Fig. 4). However, just as for the two theories discussed above, there is a quantitative disagreement on the values of the exponents.

Note that the Pr at which the crossover of the boundary layer thicknesses occurs depends on Ra. At a constant Pr, the boundary layer thicknesses decrease with increasing Ra (Fig. 5). This is expected because of the increase in Re and the Nu. The thermal boundary layer thickness is however decreasing faster than the viscous one. A crossover occurs at a Ra which is smaller for a larger Pr (Fig. 5). This can be rationalized as follows: The maximum of the azimuthal velocity fluctuation locates the beginning of the region in which advection becomes important. For a small Pr, thermal diffusion is more capable of keeping pace with advection and the thermal boundary layer may extend further into the bulk of the shell.

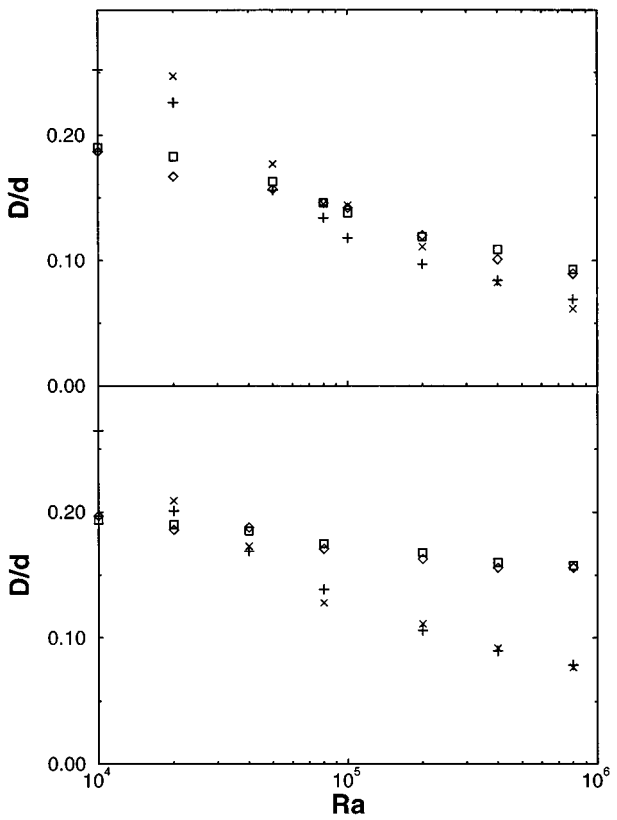

FIG. 5. Variation of the normalized boundary layer thicknesses D/d with Ra at Pr=1 (upper panel) and 10 (lower panel). Symbols are the same as in Fig. 4.

At the onset of convection, the most unstable mode is described by the spherical harmonic of order 3 which corresponds to three pairs of convection rolls in a meridional cross section. Furthermore, the ratio $2\pi<r>/d\approx7.3$, where $\langle r\rangle/d=7/6$ is the mean of the inner and outer radii of the shell. Based on the number of rolls and the effective aspect ratio of the shell, it seems appropriate to compare the numerical results with the experimental data from a cell of aspect ratio 6.7 [9,10] (Fig. 1). In cells of smaller aspect ratio, a Ra larger than 4×10^7 is required in order to observe $\mathrm{Nu}\propto\mathrm{Ra}^{2/7}$. Unfortunately, no experimental velocity measurements are available for the cell of aspect ratio 6.7. It has however been reported [9] that the Reynolds number scales at a high enough Ra at Pr=0.7 in cells of aspect ratio 1 and 0.5 as $\mathrm{Ra}^{0.485}$ and $\mathrm{Ra}^{0.49}$, respectively. A $\mathrm{Nu}\propto\mathrm{Ra}^{2/7}$ dependence was also obtained in numerical simulations of plane layers with periodic lateral boundary conditions [15,16].

Comparing the spherical model at Pr=1 with the experiments [1,3,9,12], the most striking feature remains that the 2/7 scaling of Nu is not observed, whereas the Reynolds number still scales the same; the Re scaling appears to be more sturdy. Plumes are accelerated in the bulk, i.e., away from the boundaries. Nu is, however, determined by the heat flux which has to transverse the boundary layers. It thus seems plausible that the Re scaling is less sensitive to the

boundary geometry than the Nu scaling. It cannot be ruled out that the 2/7 scaling of the Nu will be recovered at yet higher Ra.

In summary, thermal convection in spherical shells has been studied. Both the spherical model and the non-Boussinesq convection exhibit asymmetric boundary layers; however, differences between these flows have been pointed out. Theories predicting the 2/7 exponent observed in the Nu(Ra) dependence in the ''hard turbulence'' regime of convection yield a Pr dependence which is qualitatively different from the one observed in the spherical model. The present work should therefore provide an incentive to systematically study the Pr dependence at a high Ra in Cartesian geometry as well. A qualitatively correct picture of the Pr dependence is given by a mixing length theory. It should be noted that the observed Pr dependence of Re is stronger than any of the theories considered above predicts. The dependence of Nu on Ra is modified compared with the one observed in experiments, but the Re(Ra) scaling remains unchanged. This second scaling is more robust and thus possibly more fundamental than the 2/7 law.

The author wishes to acknowledge F. H. Busse for useful discussions. This work was supported by the ''Deutsche Forschungsgemeinschaft'' (DFG).

[1] F. Heslot, B. Castaing, and A. Libchaber, Phys. Rev. A **36**, 5870 (1987).
[2] L. N. Howard, J. Fluid Mech. **17**, 405 (1963); W. V. R. Malkus, Proc. R. Soc. London, Ser. A **225**, 185 (1954).
[3] B. Castaing, G. Gunaratne, F. Heslot, L. Kadanoff, A. Libchaber, S. Thomae, X. Z. Wu, S. Zaleski, and G. Zanetti, J. Fluid Mech. **204**, 1 (1989).
[4] B. I. Shraiman and E. D. Siggia, Phys. Rev. A **42**, 3650 (1990).
[5] A. Belmonte, A. Tilgner, and A. Libchaber, Phys. Rev. E **51**, 5681 (1995).
[6] For a recent review, see E. Siggia, Annu. Rev. Fluid Mech. **26**, 137 (1994).
[7] W. Hirsching and F. H. Busse, Geophys. Astrophys. Fluid Dyn. **72**, 145 (1993); D. Bercovici, G. Schubert, G. A. Glatzmaier, and A. Zebib, J. Fluid Mech. **206**, 75 (1989).
[8] A. Tilgner and F. H. Busse (unpublished).
[9] X. Z. Wu and A. Libchaber, Phys. Rev. A **45**, 842 (1992).
[10] X. Z. Wu, Ph.D. thesis, University of Chicago, 1991.
[11] X. Z. Wu and A. Libchaber, Phys. Rev. A **43**, 2833 (1991).
[12] M. Sano, X. Z. Wu, and A. Libchaber, Phys. Rev. A **40**, 6421 (1989).
[13] A monotonic dependence of Nu on Pr is not supported experimentally, either. See A. Belmonte, A. Tilgner, and A. Libchaber, Phys. Rev. E **50**, 269 (1994); S. Globe and D. Dropkin, J. Heat Transfer **81**, 24 (1959).
[14] R. H. Kraichnan, Phys. Fluids **5**, 1374 (1962).
[15] S. L. Christie and J. A. Domaradzki, Phys. Fluids A **5**, 412 (1993).
[16] R. M. Kerr, J. Fluid Mech. (to be published).